Structural order effect in visible photoluminescence properties of nanocrystalline Si:H thin films

H. Chen and W. Z. Shen[a)]

Laboratory of Condensed Matter Spectroscopy and Opto-Electronic Physics, Department of Physics, Shanghai Jiao Tong University, 1954 Hua Shan Road, Shanghai 200030, People's Republic of China

W. S. Wei

School of Physics and Information, Wenzhou University, Wenzhou, Zhejiang 325027, People's Republic of China

We report room-temperature visible photoluminescence (PL) properties of highly ordered hydrogenated nanocrystalline Si (nc-Si:H) with good electrical performance. The PL profiles can be well reproduced by the model of Islam and Kumar [J. Appl. Phys. **93**, 1753 (2003)], incorporating the effects of quantum confinement and localized surface states, as well as a log-normal crystallite size distribution. Raman, PL, and electrical results consistently reveal that improvement of structural order within nc-Si:H is beneficial to enhance the PL efficiency. Owing to adequate order, strong visible PL and high electron mobility can coexist in nc-Si:H, which may provide possibilities in Si-based optoelectronics. © *2006 American Institute of Physics*. [DOI: 10.1063/1.2189116]

Silicon nanostructures (NSs), where Si nanocrystals are embedded in matrix materials varying from SiO_2 (Ref. 1), silicon nitride (Ref. 2), to amorphous Si:H (*a*-Si:H) (Refs. 3 and 4), have received great attention in the past few decades due to their importance in fundamental physics and potential applications to optoelectronic devices such as light emitting diodes,[5] optical memories,[6] solar cells,[3] thin film transistors,[7] and single electron transistors.[8] The mechanism responsible for the visible photoluminescence (PL) in these Si NSs observed at room temperature is not fully understood, although numerous models have been proposed, including quantum confinement effect (QCE), surface states, *a*-Si:H, surface hydrides, defects in the oxide, and even specific chemical species such as siloxenes.[2,5,9] It is generally accepted that owing to the breakdown of translation invariance in Si NSs, the QCE in Si nanocrystals opens up the band gap and relaxes the **k**-conservation rule for radiative transitions,[10] giving rise to visible PL for crystallite sizes below ~5 nm; and that amorphous Si rather than crystalline Si(*c*-Si) can exhibit efficient near-infrared or visible PL. Thus it is natural to exaggerate the disorder reminiscent of positive role in the visible PL of Si NSs. The question arises concerning what is the effect of structural order in Si NSs on their visible PL properties?

On the other hand, it is worth noting that the electrical properties of the Si NSs are commonly poor, i.e., carrier mobility does not exceed the order of 10 cm²/V s (Refs. 1, 3, and 4), and carrier transport between nanocrystals (i.e., grains) is prohibited in many cases.[1] It seems plausible that the intense PL occurs at the price of good electrical properties in the Si NSs. Very recently, we have realized highly ordered hydrogenated nanocrystalline Si(nc-Si:H) thin films (where Si nanocrystals are embedded in *a*-Si:H) on both *p*- and *n*-type lattice-matched *c*-Si substrates under optimized conditions by plasma-enhanced chemical vapor deposition (PECVD), and reported good electrical properties via magnetic-field-dependent Hall measurements and mobility

spectrum analysis.[11,12] The corresponding room-temperature electron mobility and dark conductivity of the nc-Si:H films can reach in the order of 10^2 cm²/V s and 10 S cm⁻¹, respectively,[11,12] which are favorable for fabricating high-speed devices. We have further observed quantum resonant tunneling due to the electronic transport through zero- and two-dimensional states in these nc-Si:H/*c*-Si heterostructures.[13] In this letter, we report the room-temperature visible PL properties of these lightly phosphorus doped nc-Si:H thin films, with the emphasis on the structural order effect and the relationship with the electrical behavior.

Two typical series [S series: S1–S4, deposited under different radio frequency (rf) powers; D series: D1–D4, deposited under different phosphorus doping ratios (PH_3/SiH_4) C_P] of *n*-type nc-Si:H thin films employed for the current study were prepared in an rf (13.56 MHz) capacitive coupled PECVD system from silane (SiH_4) and hydrogen (H_2), with phosphine (PH_3) as dopant gas. The detailed deposition parameters are summarized in Table I. Unpolarized Raman scattering (in backscattering configuration) and PL spectra were performed on the same sample spots at room temperature on a Jobin Yvon LabRAM HR 800 UV micro-Raman spectrometer using 514.5 nm line from an Ar⁺ laser. Care was taken to avoid sample heating due to the incident laser beam.

TABLE I. Deposition parameters for the two series of lightly P-doped nc-Si:H thin films. C_P is the phosphorus doping ratio (PH_3/SiH_4), R_H is the hydrogen dilution ratio [$H_2/(H_2+SiH_4)$], and T_S is the substrate temperature.

Samples		rf Power (W)	C_P (%)	Chamber pressure (Torr)	R_H (%)	T_S (°C)	Substrate
S series	S1	30	0.8	1.0	99.0	250	*c*-Si
	S2	45	0.8	1.0	99.0	250	*c*-Si
	S3	75	0.8	1.0	99.0	250	*c*-Si
	S4	90	0.8	1.0	99.0	250	*c*-Si
D series	D1	60	0	0.7	99.0	250	*c*-Si
	D2	60	1.0	0.7	99.0	250	*c*-Si
	D3	60	5.0	0.7	99.0	250	*c*-Si
	D4	60	10.0	0.7	99.0	250	*c*-Si

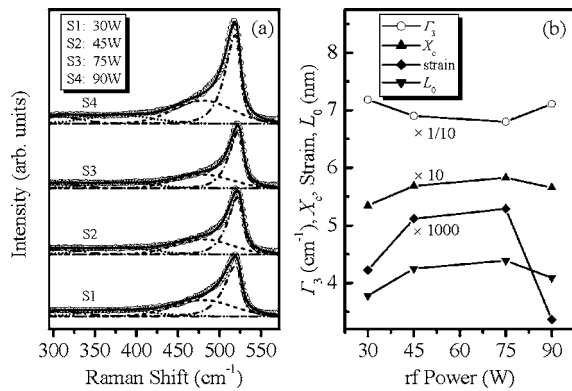[a)]Author to whom correspondence should be addressed; electronic mail: wzshen@sjtu.edu.cn

FIG. 1. (a) Experimental (open circles) and calculated (solid curves) Raman spectra, which are shifted vertically for clarity, for samples S1–S4, and (b) the resulting FWHM Γ_3 of amorphous transverse optical band at 480 cm^{-1}, crystallinity X_c, intrinsic compressive strain, and average grain size L_0.
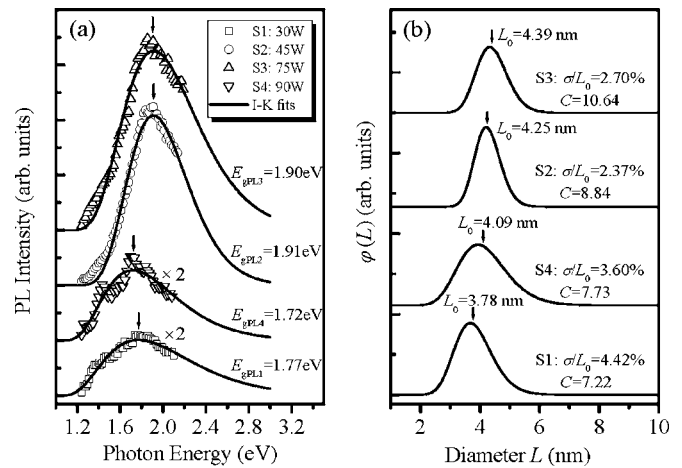

FIG. 2. (a) Experimental (open scatters) and calculated (solid curves) PL spectra, which are shifted vertically for clarity, of samples S1–S4, and (b) the derived $\varphi(L), \sigma/L_0$, together with the QC-related parameter C.

We start with Raman analyses for deducing order-related microstructural information of samples S1–S4. As shown in Fig. 1(a), the experimental Raman spectra (open circles) are decomposed into three Gaussian phonon bands [i.e., longitudinal acoustic band centered at 300 cm^{-1}, longitudinal optical band at 380 cm^{-1}, and transverse optical (TO$_1$) band at 480 cm^{-1}] from the amorphous Si contribution, and one asymmetric transverse optical (TO$_2$) band at $\sim$520 cm^{-1} from the crystalline Si contribution calculated by the strain-incorporated three-dimensional phonon confinement model.[14] Good agreement has been achieved between the calculated (solid curves) and experimental Raman spectra. The crystallinity X_c can be obtained by using $X_c = I_{TO_2}/(I_{TO_2} + \gamma I_{TO_1})$, where $\gamma(L_0) = 0.1 + \exp(-L_0/25)$ with L_0 the average defect distance in units of nm, and I_{TO_1} and I_{TO_2} are integrated intensities of TO$_1$ and TO$_2$ bands, respectively.[15] Figure 1(b) displays the resultant full width at half maximum (FWHM) Γ_3 of TO$_1$ band, X_c, L_0, and intrinsic compressive strain for these nc-Si:H. The yielded L_0 (3.8–4.5 nm for S1–S4), which are consistent with grain size results (3.6–4.9 nm) deduced from the x-ray diffraction experiments, can be regarded as the average grain sizes for the nc-Si:H. Γ_3, being linearly proportional to bond-angle variation in an a-Si:H network, is indicative of the degree of short-range order.[16] The results of Γ_3, X_c, and L_0 consistently indicate that increasing rf power first enhances and then reduces the degree of structural order within these n-type nc-Si:H.

Figure 2(a) shows the room-temperature visible PL spectra for samples S1–S4, revealing that the PL intensities of S2 and S3 (with peak energies $E_{gPL2} = 1.91$ eV and $E_{gPL_3} = 1.90$ eV) are larger by a factor of $\sim$10 than those of S1 and S4 (with $E_{gPL1} = 1.77$ eV and $E_{gPL4} = 1.72$ eV). The PL profiles can be well reproduced by using the model (solid curves) of Islam and Kumar[10] (denoted as the I-K model hereafter), which incorporates the effects of both quantum confinement (QC) and localized surface states (LSS), together with a log-normal rather than normal distribution of grain sizes (the normal distribution case is excluded here for yielding unreasonable fitting results). According to the I-K model, band gap widening ΔE due to QCE is modeled as $\Delta E = C/L^q$, where C and q are constants, and L (in nm) is the Si nanocrystallite diameter. The log-normal size distribution function $\varphi(L)$ is given in Ref. 10, with the size dispersion σ/L_0 included. During the PL profile simulation, we only

vary σ and C, and use the Raman-yielded L_0 values and take $q = 2$ in terms of effective mass theory,[2] with the other fitting parameters remaining unchanged as in Ref. 10 for hydrogen passivated Si nanocrystals. The resulting $\varphi(L)$, σ/L_0, and QC-related parameter C are shown in Fig. 2(b). The σ/L_0 value first decreases and then increases with increasing rf power, which further confirms that S2 and S3 are more ordered than S1 and S4. As σ/L_0 increases, the PL spectra broaden in these nc-Si:H accompanied by a decrease in the PL intensity. The rf power dependent behavior of C in opposite to σ/L_0 implies that QCE enhances with the improvement of the structural order within these nc-Si:H. This satisfactorily explains why samples S2 and S3 with slightly larger grain sizes have larger PL peak energies than S1 and S4.

Let us then discuss the rationality of the I-K model employed here. Aside from the well recognized QCE in Si NSs, localized surface states or defects, such as hydrides or Si dangling bonds around nanocrystals also influence the PL peak energy and profile. In addition, the surface-to-volume ratio increases as the grain size decreases, the influence of surface states on the PL from smaller nanocrystals will be highly enhanced.[10] The QC model without considering the effect of LSS (Ref. 9) alone cannot well reproduce the experimental PL spectra for S1–S4. On the other hand, temperature-dependent PL measurements for samples S1–S4 reveal that the PL peak energy redshifts by $\sim$60 meV and PL intensity decreases when the temperature is elevated from 83 to 303 K. The corresponding temperature coefficient of band gap is determined to be -2.7×10^{-4} eV/K, which is strikingly close to that of c-Si (-2.6×10^{-4} eV/K) (Ref. 17), suggesting that radiative recombination occurs mainly within Si nanocrystals. These results further corroborate the PL mechanism of these nc-Si:H.

In order to gain more insight into the microstructure of these nc-Si:H, we correlate the Raman and PL results with the electrical ones. Since the average grain size L_0 is indicative of structural order, we plot C, Γ_3, X_c, and σ/L_0 vs L_0 in Fig. 3(a), and the room-temperature electron mobility μ, as well as the PL peak intensity I_{peak} and integral intensity $I_{integral}$ vs L_0 in Fig. 3(b). It is clear that with increasing L_0, Γ_3 and σ/L_0 decrease while X_c and C increase, confirming the consistency between the Raman and PL analyses in terms of structural order. The μ of samples S1–S4 has been
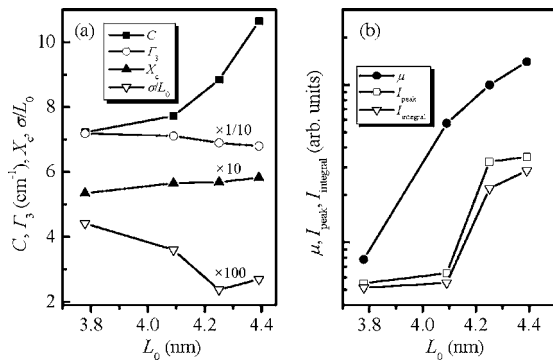
FIG. 3. (a) Parameters C, Γ_3, X_c, σ/L_0 deduced from the Raman and PL analyses, and (b) room-temperature electron mobility μ, as well as the PL peak intensity I_{peak} and integral intensity I_{integral}, vs the average grain size L_0 for samples S1–S4.

explained[11] in terms of the grain-boundary barrier controlled carrier transport model.[18] More specifically, the degradation of mobility is related to the increase of the barrier height and width.[11] Therefore, μ is believed to reflect phenomenologically the degree of order within the nc-Si:H. The enhancement of μ with increasing L_0 [Fig. 3(b)] demonstrates the above argument and also the validity of the Raman and PL analyses.

Of particular interest is that both the PL intensity and μ roughly enhances with the increase of order as implied by Fig. 3(b), varying by about one order of magnitude, which indicates the coexistence of strong visible PL and high electron mobility in these lightly doped nc-Si:H. Meanwhile, the influence of varying the rf power (30–90 W) on the structural order can be well elucidated by the competition between hydrogen chemical annealing and ion bombardment induced amorphization during the growth of nc-Si:H (Ref. 7).

More evidence for the effect of structural order on the visible PL properties is also found in samples D1–D4. Similar Raman, PL, and electrical analyses for samples S1–S4 are also applicable to D1–D4, revealing that the electron mobility increases with the decrease of barrier height and width.[12] In Fig. 4, we simply show the experimental and calculated PL spectra for these nc-Si:H, as well as the variation of Γ_3, C, X_c, L_0, σ/L_0, μ, I_{peak}, and I_{integral} with C_P, which again

indicate that the increase of structural order is helpful to enhance the visible PL efficiency.

Above results highlight the effect of structural order on the band-edge PL properties in the Si NSs, which is expected in part by the I-K model itself:[10] although the PL peak energy is dominantly determined by L_0, less σ/L_0 (i.e., more ordered) will lead to a blueshift of PL peak, an increase of PL intensity, and narrowing of the PL spectrum for a given L_0; the increase of the surface states related order is also beneficial to enhance the PL intensity, owing to the reduction of nonradiative centers.

Finally, we return to discuss the foregoing lightly doped nc-Si:H. The strong visible PL and high μ are found to coexist due to adequate order. One would ask that why does not c-Si exhibit efficient luminescence from the viewpoint of structural order? The origin lies in the absence of Si NSs in c-Si regardless of its even higher order. Notice that the Si nanocrystals in the Si NSs should be neither too small to let carrier transport,[18] nor too large to produce visible luminescence and considerable oscillator strength f.[10] Also, the magnitudes of QCE and f are affected by the surrounding medium around the nanocrystals.[10] Therefore, the "tradeoff" between the improvement of structural order and the creation of visible luminescent Si NSs, by controlling growth conditions such as gas pressure, hydrogen dilution ratio, and substrate temperature (they are not independent of each other for optimizing the growth of nc-Si:H), and/or by post-treatment such as appropriate annealing or hydrofluoric acid dipping, will facilitate to deposit nc-Si:H with both strong visible luminescent and good electrical properties, which may provide possibilities in Si-based optoelectronics.
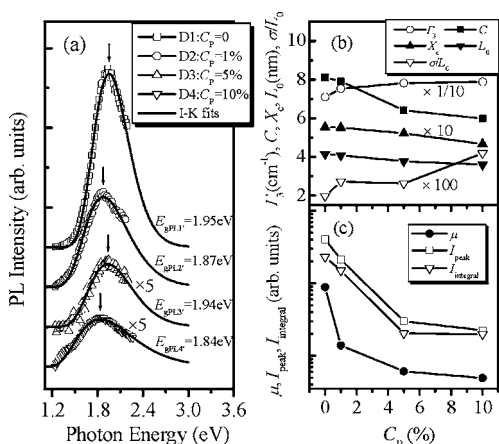
FIG. 4. (a) Experimental (open scatters) and calculated (solid curves) PL spectra, which are shifted vertically for clarity, of samples D1–D4. (b) The relevant Γ_3, C, X_c, L_0, σ/L_0, and (c) room-temperature electron mobility μ, as well as the PL peak intensity I_{peak} and integral intensity I_{integral}, vs C_P for D1–D4.

[1]M. Fujii, A. Mimura, S. Hayashi, and K. Yamamoto, Appl. Phys. Lett. **75**, 184 (1999).
[2]T. Y. Kim, N. M. Park, K. H. Kim, G. Y. Sung, Y. W. Ok, T. Y. Seong, and C. J. Choi, Appl. Phys. Lett. **85**, 5355 (2004).
[3]A. Shah, P. Torres, R. Tscharner, N. Wyrsch, and H. Keppner, Science **285**, 692 (1999); I. C. Cheng and S. Wagner, Appl. Phys. Lett. **80**, 440 (2002).
[4]H. Chen, M. H. Gullanar, and W. Z. Shen, J. Cryst. Growth **260**, 91 (2004).
[5]A. G. Cullis, L. T. Canham, and P. D. J. Calcott, J. Appl. Phys. **82**, 909 (1997).
[6]R. J. Walters, P. G. Kik, J. D. Casperson, H. A. Atwater, R. Lindstedt, M. Giorgi, and G. Bourianoff, Appl. Phys. Lett. **85**, 2622 (2004).
[7]B. Kalache, A. I. Kosarev, R. Vanderhaghen, and R. Roca i Cabarrocas, J. Appl. Phys. **93**, 1262 (2003).
[8]U. Meirav, M. Kastner, and S. J. Wind, Phys. Rev. Lett. **65**, 771 (1990).
[9]P. F. Trwoga, A. J. Kenyon, and C. W. Pitt, J. Appl. Phys. **83**, 3789 (1998).
[10]M. N. Islam and S. Kumar, J. Appl. Phys. **93**, 1753 (2003).
[11]X. Y. Chen, W. Z. Shen, and Y. L. He, J. Appl. Phys. **97**, 024305 (2005).
[12]X. Y. Chen and W. Z. Shen, Phys. Rev. B **72**, 035309 (2005).
[13]X. Y. Chen and W. Z. Shen, Appl. Phys. Lett. **85**, 287 (2004).
[14]M. Yang, D. M. Huang, P. H. Hao, F. L. Zhang, X. Y. Hou, and X. Wang, J. Appl. Phys. **75**, 651 (1994).
[15]E. Bustarret, M. A. Hachicha, and M. Brunel, Appl. Phys. Lett. **52**, 1675 (1988).
[16]D. X. Han, J. D. Lorentzen, J. Weinberg-Wolf, L. E. McNeil, and Q. Wang, J. Appl. Phys. **94**, 2930 (2003).
[17]Z. Yang, K. P. Homewood, M. S. Finney, M. A. Harry, and K. J. Reeson, J. Appl. Phys. **78**, 1958 (1995).
[18]T. Weis, R. Lipperheide, U. Wille, and S. Brehme, J. Appl. Phys. **92**, 1411 (2002).